Activation of Dual Oxidases Duox1 and Duox2

DIFFERENTIAL REGULATION MEDIATED BY cAMP-DEPENDENT PROTEIN KINASE AND PROTEIN KINASE C-DEPENDENT PHOSPHORYLATION*[S]

Sabrina Rigutto[‡1,2], **Candice Hoste**[‡2], **Helmut Grasberger**[§3], **Milutin Milenkovic**[‡], **David Communi**[‡4], **Jacques E. Dumont**[‡], **Bernard Corvilain**[‡¶], **Françoise Miot**[‡], and **Xavier De Deken**[‡5]

From the ‡*Institut de Recherche Interdisciplinaire en Biologie Humaine et Moléculaire and the* ¶*Department of Endocrinology, Hôpital Erasme, Université Libre de Bruxelles, Campus Erasme, 1070 Brussels, Belgium and the* §*Department of Medicine, University of Chicago, Chicago, Illinois 60637*

Dual oxidases were initially identified as NADPH oxidases producing H_2O_2 necessary for thyroid hormone biosynthesis. The crucial role of Duox2 has been demonstrated in patients suffering from partial iodide organification defect caused by biallelic mutations in the *DUOX2* gene. However, the Duox1 function in thyroid remains elusive. We optimized a functional assay by co-expressing Duox1 or Duox2 with their respective maturation factors, DuoxA1 and DuoxA2, to compare their intrinsic enzymatic activities under stimulation of the major signaling pathways active in the thyroid in relation to their membrane expression. We showed that basal activity of both Duox isoenzymes depends on calcium and functional EF-hand motifs. However, the two oxidases are differentially regulated by activation of intracellular signaling cascades. Duox1 but not Duox2 activity is stimulated by forskolin ($EC_{50} = 0.1 \ \mu M$) via protein kinase A-mediated Duox1 phosphorylation on serine 955. In contrast, phorbol esters induce Duox2 phosphorylation via protein kinase C activation associated with high H_2O_2 generation (phorbol 12-myristate 13-acetate $EC_{50} = 0.8$ nM). These results were confirmed in human thyroid cells, suggesting that Duox1 is also involved in thyroid hormonogenesis. Our data provide, for the first time, detailed insights into the mechanisms controlling the activation of Duox1–2 proteins and reveal additional phosphorylation-mediated regulation.

Dual oxidases (Duox1 and Duox2) belong to the family of NADPH oxidases (Nox), which is composed of five additional

enzymes: Nox1–5 (1–3). These transmembrane proteins are characterized by a COOH-terminal NADPH oxidase catalytic core responsible for reactive oxygen species synthesis. The best characterized NADPH oxidase Nox2 is involved in the leukocyte respiratory burst and activated by invading pathogens (4). The mechanisms controlling the Nox-mediated reactive oxygen species production are multiple and complex. The activation of Nox1 (5, 6), Nox2 (3, 7), and Nox3 (8, 9) requires the coordinated assembly of several subunits: the association with the transmembrane protein p22*phox* and the recruitment of three cytosolic proteins, the small G protein Rac, p47*phox* (or NOXO1), and p67*phox* (or NOXA1).

Duox1 and Duox2 isoenzymes are large members of the Nox/Duox family. In addition to the catalytic core, Duox1 and Duox2 proteins are NH_2-terminally extended by an extracellular peroxidase-like domain followed by a membrane-spanning segment and an intracellular domain comprising two canonical EF-hand motifs (2). Duox1 and Duox2 are the sole proteins directly generating H_2O_2 (10) outside the cells, whereas small Nox homologues are mostly superoxide generators (3). Duox isoforms do not need to be associated with cytosolic factors to be active but undergo a critical maturation process necessary to acquire their active conformation at the apical cell surface of the thyrocytes (11). The immature nonfunctional form (180 kDa) is not properly glycosylated and maintained in the endoplasmic reticulum compartment. Only the co-expression of the Duox maturation factors (DuoxA1 and DuoxA2) allows functional reconstitution. They are *N*-glycosylated proteins permitting the endoplasmic reticulum exit of properly folded Duox enzymes (12, 13). The *DUOXA* genes are localized near their respective *DUOX* gene in a head to head orientation on chromosome 15 and co-expressed with their Duox counterpart in the same tissues (12).

Dual oxidases expressed at the apical side of surface epithelia exposed to microorganisms, like the airways or the digestive tract, are supposed to function as components of the innate host defense system (14–16). However, Duox1 and Duox2 isoenzymes were initially identified as H_2O_2-generating thyroid oxidases (1, 2). The main function of the thyroid is the uptake and concentration of iodide from the bloodstream to synthesize thyroid hormones (T3 and T4) in the follicular lumen (17). H_2O_2 produced at the apical pole of the thyrocyte is utilized by thyroperoxidase as an electron acceptor to oxidize iodide, covalently link oxidized iodide to tyrosines of thyroglobulin,

and couple iodinated tyrosyl residues to form protein-bound iodothyronines (T3 and T4) (18). Under physiological iodide supply, hormonogenesis is rate-limited by the availability of hydrogen peroxide (19). Patients presenting iodide organification defect caused by mutations in their *DUOX2* gene suffer from transient or permanent hypothyroidism depending on the mono- or bi-allelic character of the mutation, demonstrating the crucial function of Duox2 in thyroid hormone synthesis (20–25). However, the physiological meaning of the co-existence of the two dual oxidases and their respective maturation factors in the thyroid tissue remains an open question.

In this study, we analyzed the mechanisms of activation of Duox1 and Duox2 using Duox/DuoxA co-transfected cells stimulated by agonists known to regulate the thyroid metabolism (26, 27). Our results indicate that Duox1 and Duox2 activities are mainly calcium-dependent NADPH oxidases. Moreover, additional mechanisms governing their intrinsic activity are different; Duox1 is positively regulated by the cAMP-dependent protein kinase A (PKA)[6] cascade, whereas Duox2 is highly induced by activation of protein kinase C (PKC) with very low concentrations of PMA.

EXPERIMENTAL PROCEDURES

Plasmids and Mutagenesis—The wild type untagged versions of human Duox1 (accession number AF230495) and Duox2 (accession number AF230496) cDNA were cloned from ATG to stop codon into the vector pcDNA3 (Invitrogen). The NH_2-terminal hemagglutinin epitope-tagged human Duox2 (HA-Duox2-pcDNA3.1) and the COOH-terminal c-Myc epitope-tagged human DuoxA1 and DuoxA2 (DuoxA1-Myc-pcDNA3.1 and DuoxA2-Myc-pcDNA3.1) were described elsewhere (12). We added an additional Rho tag to Duox1 to be able to distinguish it from HA-Duox2 in future experiments. The Duox1 native signal peptide was replaced by the TSH receptor signal peptide to facilitate the cloning step. The Rho-HA-Duox1-pcDNA3 construct was generated as follows. The 23 first amino acids (residue 1 corresponding to the initiation methionine) of the human Duox1 protein (accession number AAF73921) were replaced by the signal peptide of the human TSH receptor (MRPADLLQLVLLLDL-PRDLGG) (accession number CAA02195) and the first 19 residues of the bovine rhodopsin (Rho) (accession number P02699) (MNGTEGPNFYVPFSNKTGVV; two putative glycosylation sites are underlined) (28). The cDNA corresponding to the NH_2-terminal HA-tagged Duox1 protein (24–1551 amino acids) was cloned just downstream of the Rho tag by insertion of an EcoRI site. The presence of the TSH receptor signal peptide, Rho, and HA tags at the NH_2 terminus of Duox1 did not affect its expression nor its peroxide generating activity (supplemental Fig. S1). Furthermore, the extra *N*-linked sugars present on the Rho tag have been very useful to separate the two glycosylated forms of Duox1 for mass spectrometry analysis, because it is mainly the mature highly glycosylated form of Duox1 that is phosphorylated upon stimulation.

Mutations in Duox1–2 were introduced by directed mutagenesis with the QuikChange system (Stratagene, La Jolla, CA) (primers are described in supplemental Table S1). All of the constructs were verified by Big Dye Terminator cycle sequencing on an automated ABI Prism 3100 sequencer (Applied Biosystems, Foster City, CA).

Cell Culture and Transfection—Cos-7 cells were cultured in Dulbecco's modified Eagle's medium (Invitrogen) with 10% fetal bovine serum (Invitrogen), 2% streptomycin-penicillin, 1% fungizone, and 1% sodium pyruvate. For H_2O_2 assay, adherent cells at 50–60% confluence were transfected in 6-well plates using FuGENE 6 reagent (Roche Applied Science) according to the manufacture's protocol (ratio: 1 μg of DNA for 3 μl of FuGENE 6) with 500 ng of Rho-HA-Duox1-pcDNA3 and 500 ng of DuoxA1-Myc-pcDNA3.1 or with 500 ng of HA-Duox2-pcDNA3.1 and 500 ng of DuoxA2-Myc-pcDNA3.1. Under optimal conditions, the transfection efficiency reached 20–30% of cells expressing Duox proteins at the cell surface detected by FACS. For immunoprecipitation experiments, the cells seeded in 10-cm-diameter dishes were transfected with 8 μg of DNA and 24 μl of FuGENE 6.

Human Thyroid Primary Culture—Human thyroid tissue was obtained from patients undergoing partial or total thyroidectomy for resection of solitary cold nodules or multinodular goiters. Only healthy, normal-looking, non-nodular tissue was used within 30 min after surgical removal. Thyrocytes in primary culture obtained from follicles isolated by collagenase digestion and differential centrifugation were cultured in Dulbecco's modified Eagle's medium/Ham's F-12/MCDB104 (2:1:1) medium (Invitrogen) with 1% sodium pyruvate, 40 μg/ml ascorbic acid, 5 μg/ml insulin, 2% streptomycin-penicillin, and 1% fungizone (29, 30). Thyrocytes were seeded 5 days before the assay. The protocol has been approved by the hospital ethics committee.

H_2O_2 Measurement and Flow Immunocytometry Analysis—Production of H_2O_2 was determined by the sensitive fluorimetric method of Bénard and Brault (31) slightly modified as previously described (11). The peroxide released from transfected cells (Duox1/DuoxA1 or Duox2/DuoxA2) into Krebs-Ringer-Hepes medium was accumulated in the presence of stimulating agents for 2.5 h at 37 °C. After removing the medium, cell surface expression of Duox1–2 proteins was measured by flow cytometry (FACS). Briefly, the cells detached with phosphate-buffered saline EDTA/EGTA (5 mM) were incubated sequentially with anti-HA antibody (clone 3F10; Roche Applied Science) and fluorescein-conjugated anti-rat IgG, both diluted 1/100 in phosphate-buffered saline, 0.1% bovine serum albumin. Propidium iodide (5 μg/ml) staining in the second incubation step was used to exclude damaged cells from subsequent analysis. Fluorescence was analyzed using cell sorting (FACScan; Becton Dickinson, Erembodegem, Belgium) counting 20,000 events/sample. Relative protein expression was determined by calculating the differences in total fluorescence intensity (Arbitrary Unit) between the samples and an equal-sized population of control cells expressing only Duox1 or Duox2 constructs without their respective maturation factors. Without the latter, no cell surface expression of Duox could be detected (11). H_2O_2 production was normalized to cell surface

---

[6] The abbreviations used are: PKA, cAMP-dependent protein kinase; PKC, protein kinase C; PMA, phorbol 12-myristate 13-acetate; WT, wild type; HA, hemagglutinin; TSH, thyroid-stimulating hormone; FACS, fluorescence-activated cell sorter; Fsk, forskolin; 6-MB-cAMP, N^6-monobutyryladenosine-3′,5′-cyclic monophosphate.

expression of each construct and reported as pg of H_2O_2/FACS. For cultures of human thyrocytes, H_2O_2 released over 90 min in the presence of various agents was normalized to total proteins extracted in Laemmli buffer and quantified by paper dye binding assay (ng of H_2O_2/μg of protein) (32).

Immunoprecipitation and Western Blot Analysis—Proteins were extracted in lysis buffer (10 mM Tris-HCl, pH 7.5, 150 mM KCl, 0.5% Nonidet P-40, 120 mM β-mercaptoethanol, 100 mM NaF, 2 mM EDTA, pH 8.0, 50 nM okadaic acid, 1 mM vanadate) supplemented with a mixture of protease inhibitors (Complete; Roche Applied Science) for 1 h at 4 °C. The lysate was centrifuged 15 min at 10,000 rpm, and the supernatant was pre-cleared with Sepharose beads (GE Healthcare). Duox1 complexes were immunoprecipitated with anti-Duox antibody (1/100) conjugated to Sepharose beads (2) and Duox2 proteins with monoclonal anti-HA antibody precoated on agarose beads (Clone HA-7; Sigma-Aldrich). Proteins of the immunoprecipitate were separated by SDS/PAGE and transferred to nitrocellulose as previously described (2). Phosphorylated Duox proteins were detected using a rabbit polyclonal antibody raised against phospho-(Ser/Thr) PKA substrate (1/1,000; Cell Signaling, Danvers, MA), which is directed to the phospho motif RXX(S/T). Fluorescent secondary antibodies (1/10,000; IRDye 800 anti-rabbit from LI-COR, Lincoln, NE) were used for image acquisition and quantification with the Odyssey infrared imaging system (LI-COR). The membrane was stripped and immunoblotted with the anti-Duox antibody (1/16,000) and fluorescent secondary antibodies (1/10,000; IRDye 680 anti-rabbit) to quantify total Duox proteins.

Radioactive Phosphorus Incorporation—Cells maintained 24 h in serum-free phosphate-depleted medium were incubated 2 h with 500 μCi (Cos-7) or 1mCi (thyrocytes) of [^{32}P]orthophosphate. The proteins were prepared as described above, and phosphorylated proteins were detected and quantified with a Storage Phosphor Screen (GE Healthcare) scanned with Typhoon Trio+ (GE Healthcare). Total Duox proteins for each condition were measured by Odyssey infrared imaging system coupled with the polyclonal anti-Duox antibody.

In Vitro PKA Phosphorylation Assay—Cos-7 Duox1/DuoxA1 transfected cells were cultured 24 h without serum. The proteins were prepared in lysis buffer, and Duox1 complexes were immunoprecipitated overnight with monoclonal anti-HA antibody precoated on agarose beads as described above. Immunoprecipitated proteins were incubated for 10 min at 37 °C in a 50-μl final volume that contained 20 mM Hepes, pH 7.4, 0.1 mM dithiothreitol, 10 mM MgCl$_2$, 0.1 mM [γ-^{32}P]ATP (5 μCi/tube), and 100 ng of purified catalytic subunit of protein kinase A (Calbiochem, Gibbstown, NJ). After SDS/PAGE and Western blotting, radioactive signals were quantified with Typhoon Trio+; Duox proteins were immunodetected with the anti-Duox antibody and visualized with Odyssey imaging system.

Mass Spectrometry Analysis—Cos-7 cells transfected with wild type Duox1 and DuoxA1 constructs were cultured 24 h without serum and stimulated 30 min with 10 μM forskolin. Duox1 complexes were immunoprecipitated with anti-Duox antibody as described above. Duox1 proteins were separated by 7%-polyacrylamide gel electrophoresis and stained with colloidal Coomassie Blue. After excision of the Duox gel bands, the

proteins were in-gel digested with trypsin or chymotrypsin, and the resulting peptides were extracted from the gel (33). The digested peptides were separated onto a C18 reverse phase 1 × 50 mm column (Vydac; Alltech Associates, Lokeren, Belgium) and deposited onto a stainless steel target. Mass spectrometry analysis was performed on a Quadrupole-time of flight Ultima Global mass spectrometer equipped with a matrix-assisted laser desorption ionization source (Micromass, Waters, Zellik, Belgium) calibrated using the monoisotopic masses of tryptic and chymotryptic peptides from bovine serum albumin.

Statistical Analysis—The data are presented as the means ± S.D. The results were analyzed using the unpaired Student's t test, and $p < 0.05$ was considered statistically significant (**, $p < 0.01$; ***, $p < 0.001$).

RESULTS

DuoxA-based Functional Assay to Study Duox-mediated H_2O_2 Generation—Heterologous systems combining DuoxA expression have already been successfully used to characterize Duox activity of human Duox2 natural mutants (13) and to reconstitute a functional H_2O_2-generating system in a lung cancer cell line (34). The originality of our study is to analyze the specific activity of Duox1 and Duox2 isoenzymes by normalizing the hydrogen peroxide production to the cell surface expression of the respective proteins. Insertion of an HA tag in the Duox1–2 ectodomain provides an effective means to reliably estimate Duox membrane expression and compare the activities of the two enzymes. We first validated our heterologous system: 1) Measurement of H_2O_2 produced after 1 μM ionomycin stimulation of cells transfected with Duox/DuoxA (constant DuoxA quantity, 50 ng) was proportional to the quantity of transfected Duox plasmids (25–500 ng) with a plateau reached at 250–500 ng of Duox DNA probably caused by a limited amount of DuoxA (Fig. 1*A*). 2) We observed a linear relationship between Duox-mediated H_2O_2 generation and the membrane expression of Duox as measured by FACS (Fig. 1*B*). The specific activity of both Duox enzymes was comparable, and no H_2O_2 was detected in cells expressing Duox or DuoxA alone (Fig. 1*A*). 3) We verified that the addition of the tags did not modify the expression and activity of Duox1–2 proteins (supplemental Fig. S1). In all experiments, the specific activity of the Duox enzymes is represented as the amount of H_2O_2 produced normalized to their surface expression (pg H_2O_2/FACS).

In humans, the thyroid metabolism is under the control of the phosphatidylinositol 4,5-bisphosphate cascade and the cAMP cascade (26, 27). In our functional assay, 1 μM ionomycin increased the activity of both Duox1 and Duox2 enzymes to the same level, but raising concentrations of ionomycin from 2 to 4 μM resulted in higher activity of Duox1 than Duox2 (Fig. 2*A*). The adenylate cyclase agonist, forskolin (Fsk), raised the amount of H_2O_2 generated by Duox1 but not by Duox2 with a 50% effective concentration (EC$_{50}$) of 0.1 μM (Fig. 2*B*). Moreover PMA, a PKC activator, differentially regulated activities of Duox1 and Duox2 (Fig. 2, *C* and *D*). Although micromolar concentrations of PMA were needed to increase Duox1 activity with an EC$_{50}$ of 1.8 μM, a maximal activation of Duox2 enzyme was already observed with nanomolar PMA concentrations
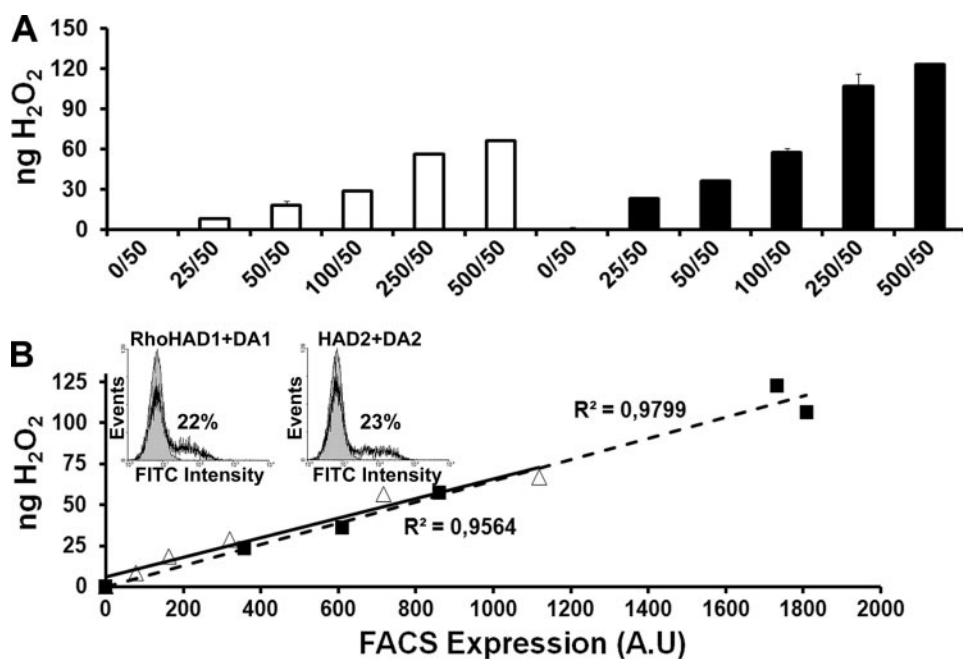
FIGURE 1. **Intrinsic activity of Duox isoenzymes in reconstituted systems.** *A*, measurement of H_2O_2 accumulation (ng) produced by Duox1/DuoxA1 or Duox2/DuoxA2 co-transfected Cos-7 cells for 2.5 h in the presence of 1 μM ionomycin. Constant amount of DuoxA-Myc-pcDNA3.1 DNA (50 ng) was transfected with increasing DNA amounts of Rho-HA-Duox1-pcDNA3 (*white*) or HA-Duox2-pcDNA3.1 (*black*) (0–500 ng). Each measurement corresponds to a transfection experiment performed in duplicate (means ± S.D.). *B*, plot of H_2O_2 production against the relative Duox expression level at the cell surface. Membrane expression of Rho-HA-Duox1 (△) and HA-Duox2 (■) proteins were quantified by FACS using the anti-HA antibody (*A.U*, arbitrary unit of fluorescein isothiocyanate fluorescence intensity). *Inset*, representative histograms of a FACS experiment; the *gray areas* represent cells transfected with the Duox construct alone. The percentage of cells expressing Duox at the cell surface is indicated for each construct.

(EC_{50} = 0.8 nM). The addition of Fsk or PMA to ionomycin in the incubation medium provoked a release of H_2O_2 corresponding to the sum of the amounts generated by the cells treated with the agents separately (Iono *versus* Iono+Fsk for Duox1: $p < 0.01$; Iono *versus* Iono+PMA for Duox1: $p < 0.001$; Iono *versus* Iono+PMA for Duox2: $p < 0.01$) (Fig. 2*E*). In contrast to Duox1, raising calcium concentration was not sufficient to activate Duox2 by Fsk. In all of the conditions, 1 μM diphenyleneiodonium, a flavoprotein inhibitor, reduced the H_2O_2 level produced by the two enzymes, indicating that it derives from an NADPH oxidase (data not shown).

Regulation of Duox Activity by Calcium—Duox-mediated H_2O_2 generation is presumed to be regulated by binding of Ca^{2+} to the two EF-hand motifs, located in the cytosolic portion spanning transmembrane domain 1 and 2 (13, 34, 35). Indeed, the absence of calcium ions in the H_2O_2 measurement assay abolished the Duox1–2 activity (data not shown). The other calcium-dependent NADPH oxidase, NOX5, possesses four calcium-binding sites arranged in two functional pairs (36). To study the role of the two Duox EF-hands, the crucial glutamate residue was replaced by a glutamine in the twelfth position of the EF-hand sequence. Duox2 mutants E843Q and E879Q completely lost the ability to produce H_2O_2 in basal or stimulated conditions but maintained a cell surface expression similar to the wild type (WT) protein (Fig. 3). Similarly, inactivation of one of the two EF-hands in Duox1 (E839Q and E875Q Duox1 mutants) was sufficient to inactivate Duox1, although a correct processing to the membrane occurred as for Duox2

(supplemental Fig. S2). These results strongly suggest that the two EF-hand motifs operate as one functional pair necessary for Duox activation in response to an increase of intracellular calcium concentration.

Duox1 Activity Is Positively Modulated through the cAMP Pathway—As shown in Fig. 2, Duox1-dependent H_2O_2 generation was positively controlled by Fsk, contrary to Duox2. To establish the role of the protein kinase A, N^6-monobutyryladenosine-3′,5′-cyclic monophosphate (6-MB-cAMP), a site-selective PKA agonist, was used. H_2O_2 produced by Duox1 was significantly increased with either 50 μM 6-MB-cAMP or 1 μM Fsk (Fig. 4*A*). We also co-transfected a vector encoding the α isoform of the PKA catalytic subunit with WT Duox/DuoxA constructs (37, 38). Overexpression of PKA for 48 h, verified by Western blotting (data not shown), also induced an increase of Duox1 activity. Co-expression of the PKA subunit had only a minor effect on Duox2 activity, and treatment with the 6-MB-cAMP did not increase H_2O_2 production by Duox2.

Motif scanning for PKA substrates based on the consensus sequence (R/K)2X(S/T) identifies three potential PKA phosphorylation sites in Duox1 (Ser^{955}, Thr^{1007}, and Ser^{1217}) (supplemental Fig. S3). We analyzed the Duox1 phosphorylation state with an anti-RXX(pS/pT) antibody that could potentially recognize phosphorylation on Ser^{955} and Ser^{1217} but not on Thr^{1007}. Under basal conditions, the mature form of Duox1 (200 kDa) was already phosphorylated in Cos-7 cells (supplemental Fig. S4). It is noteworthy that the slower migrating form of Duox1 (mature form) and the immature form were shifted to 200 and 190 kDa, respectively, instead of the wild type 190- and 180-kDa proteins. This phenomenon can be explained by the addition of extra N-linked sugars on the two putative N-glycosylation sites present in the Rho tag sequence as previously described for similar TSH receptor constructs (28). Duox1 phosphorylation was stimulated by Fsk in a time-dependent way with a maximum reached after 30 min of stimulation (supplemental Fig. S4). Increased Duox1 phosphorylation was also observed in cells treated 30 min with 6-MB-cAMP or cells overexpressing the PKA catalytic subunit (Fig. 4*B*). The stimulatory effect of Fsk was also observed on H_2O_2 accumulation for 30 min (data not shown). Constitutive and PKA-induced phosphorylation of Duox1 was evident, in ^{32}P incorporation experiments, with the detection of a major radioactive band corresponding to the high molecular mass form (200 kDa) of Duox1 (supplemental Fig. S5). No increase of Duox2 phosphorylation
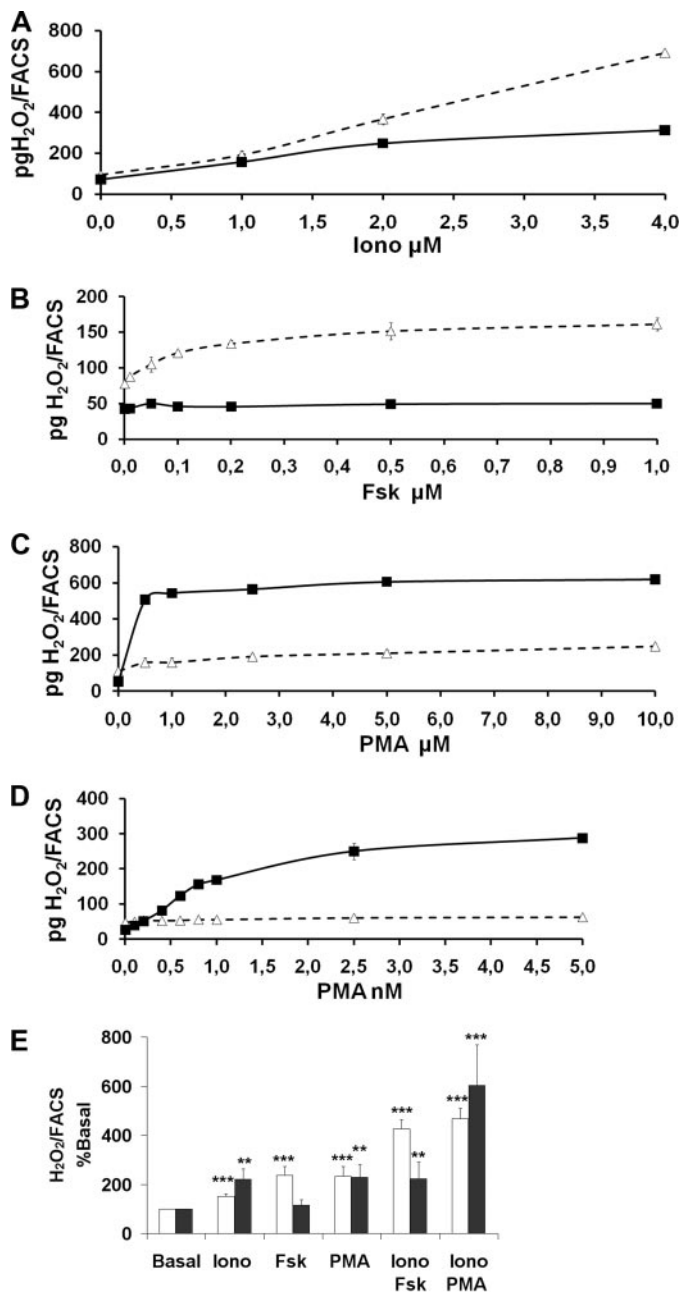
FIGURE 2. **H$_2$O$_2$ generation in response to ionomycin, Fsk, or PMA.** Measurement of H$_2$O$_2$ produced by Cos-7 cells co-expressing Rho-HA-Duox1/DuoxA1 (△) or HA-Duox2/DuoxA2 (■) for 2.5 h normalized to Duox membrane expression. The cells were stimulated during the 2.5-h period with increasing concentrations of ionomycin (*A*), Fsk (*B*), or PMA (*C* and *D*). Each measurement corresponds to a transfection experiment performed in duplicate (means ± S.D.). *E*, H$_2$O$_2$ production of Cos-7 cells co-expressing Rho-HA-Duox1/DuoxA1 (*white*) or HA-Duox2/DuoxA2 (*black*) stimulated during the 2.5-h period with 1 μM ionomycin in combination with 1 μM Fsk or PMA (5 μM for Duox1 and 0.5 nM for Duox2). H$_2$O$_2$ produced in basal condition was considered as 100% (means ± S.D., *n* = 4). Statistical significances compared with basal are indicated. **, *p* < 0.01; ***, *p* < 0.001.

could be detected under Fsk stimulation by ^{32}P incorporation experiments (data not shown).

Identification of PKA Target Sites in Duox1—To identify the phosphorylated sites by PKA, Duox1 protein was isolated from Fsk-stimulated Cos-7 cells co-transfected with Duox1/DuoxA1 and subjected to mass spectrometry analysis. After trypsin or chymotrypsin digestions, two phosphorylated peptides were
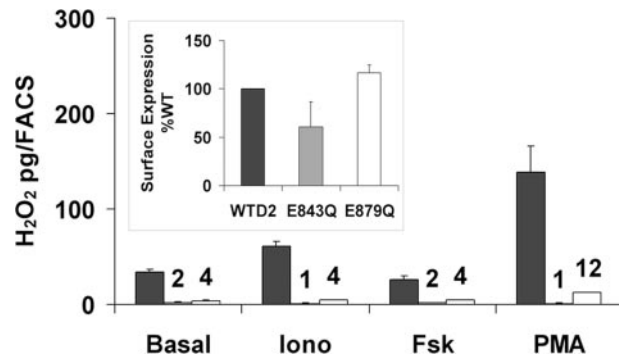

FIGURE 3. **Loss of Duox2 activity by mutations in EF-hand motifs.** H$_2$O$_2$ accumulation was performed for 2.5 h at 37 °C in the presence of 1 μM ionomycin (*Iono*), 1 μM Fsk, or 1 nM PMA from cells expressing DuoxA2 with wild type (*black*), E843Q (*gray*), or E879Q (*white*) HA-Duox2. The graphs show the means ± S.D. (*n* = 4). Expression of mutated Duox2 constructs at the cell surface relative to WT is shown in the *inset*.

isolated and microsequenced: the peptide [954]A*S*YISQDMICP-SPR[967], which encloses the serine 955 (underlined), and the peptide [1214]RRR*S*FRGF[1221] including the serine 1217. Three peptides containing the threonine 1007 ([1006]V*T*SFQPLL-FTEAHREK[1021], [1005]KV*T*SFQPLLFTEAHR[1019], and [1006]V*T*S-FQPLLFTEAHR[1019]) were also isolated but were not phosphorylated.

To address the role of these potential phosphorylated residues in Duox1 activity, we replaced them with the nonphosphorylatable amino acid, alanine. Three single mutants (S955A, T1007A, and S1217A) and one double mutant (S955A/S1217A) were constructed. Cos-7 cell surface expression of T1007A and S1217A mutants was similar to membrane expression of WT protein, whereas S955A and S955A/S1217A were less expressed than the WT Duox1 (Fig. 5*A*, *inset*). The basal activity of S955A Duox1 was severely impaired and was no longer stimulated after Fsk treatment, whereas it still responded to ionomycin and PMA (Fig. 5*A*). Mutant T1007A presented a slightly lower activity than the WT protein but was still positively regulated by all agonists. Interestingly, mutation S1217A generated an enzyme with increased basal activity, and the double mutant S955A/S1217A produced a similar H$_2$O$_2$ amount as WT Duox1 in basal and stimulated conditions, except for a loss of response to Fsk.

Phosphorylation state of Duox1 mutants in basal condition or after Fsk stimulation was analyzed by radioactive phosphorus incorporation (Fig. 5*B*). Basal phosphorylation of the 200-kDa mature form of S955A and S1217A Duox1 was highly decreased compared with the WT Duox1 but was still stimulated by Fsk. The T1007A mutant presented the same Fsk-dependent phosphorylation pattern as WT Duox1. On the other hand, the S955A/S1217A double mutant showed a very low basal phosphorylation no longer stimulated by Fsk. The same experiment was performed using the anti-phospho PKA substrate antibody. Unfortunately, this antibody was unable to recognize the Ser[1217] and Thr[1007] as demonstrated by the complete absence of phosphorylation of the S955A mutant (supplemental Fig. S6). Nevertheless, the results confirmed the Fsk-mediated phosphorylation of serine 955. Direct phosphorylation of Duox1 was measured *in vitro*. In the presence of purified PKA, WT and T1007A Duox1 showed robust phos-
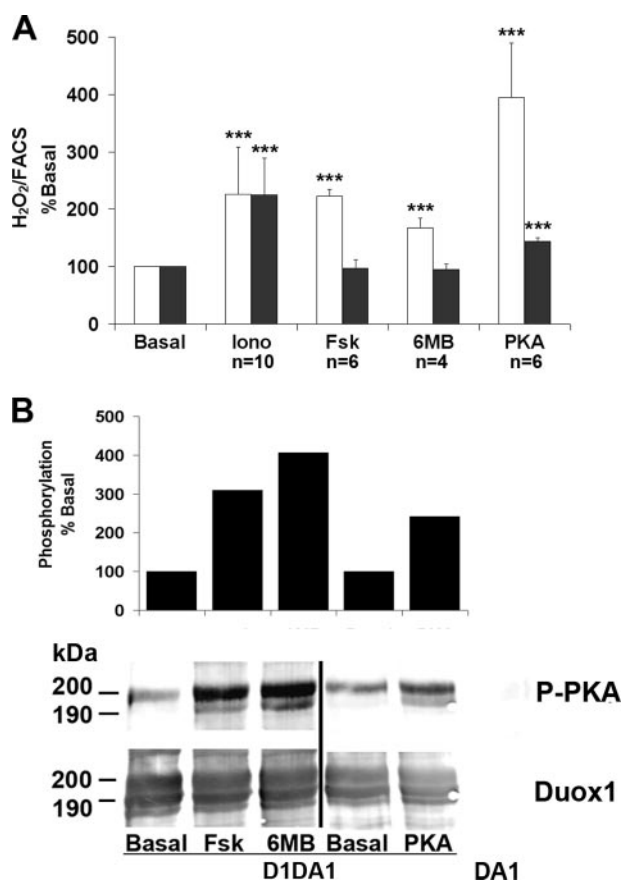
FIGURE 4. **cAMP-dependent activation of Duox1.** *A*, Cos-7 cells expressing Rho-HA-Duox1/DuoxA1 (*white*) or HA-Duox2/DuoxA2 (*black*) were stimulated for 2.5 h with 1 μM ionomycin (*Iono*), 1 μM Fsk, or 50 μM 6-MB-cAMP corresponding to the time of H_2O_2 accumulation. In the PKA condition, cells transfected with a third vector coding for the PKA catalytic subunit. H_2O_2 production was normalized to Duox cell surface expression, and the resulting specific activities are expressed relative to the basal condition (set to 100). The data are shown as the values ± S.D. for n indicated measurements (***, $p < 0.001$). *B*, immunodetection of Duox1 phosphorylation mediated by agents activating the cAMP cascade. The cells were treated for 30 min with either 1 μM Fsk or 50 μM 6-MB-cAMP. After anti-Duox immunoprecipitation, PKA phosphorylation was immunodetected with the anti-RXX(pS/pT) antibody (*P-PKA*) and total Duox1 with anti-Duox polyclonal antibody. In the *top panel*, the *columns* represent PKA-mediated Duox1 phosphorylation corrected to the total amount of immunoprecipitated Duox1. The level of phosphorylation is expressed relative to the basal phosphorylation set to 100. The PKA condition was performed in a different experiment from Fsk and 6-MB-cAMP (*6MB*).

phorylation with the appearance of an additional highly phosphorylated form corresponding to the immature 190-kDa protein (Fig. 5*C*). As expected, the PKA-dependent phosphorylation of S955A, S1217A, and S955/S1217A mutants was clearly decreased. Taken together, these results demonstrate that Ser[955] and Ser[1217] are two key residues phosphorylated by PKA controlling Duox1 activity.

Duox2 Activity Is Modulated by the PKC—We have shown that Duox2 activity was stimulated with nanomolar concentrations of PMA (Fig. 2). To determine whether PMA-dependent activation of Duox2 involves PKC-dependent phosphorylation, Cos-7 cells expressing Duox2/DuoxA2 were incubated with PKC inhibitors. One μM Ro318220 or Gö6976 specifically inhibited PMA-stimulated H_2O_2 production by 50% with no effect in basal and ionomycin stimulated conditions (Fig. 6*A*). Analysis of radioactive phosphorus incorporation showed a

time-dependent phosphorylation of Duox2, already visible after 10 min of exposure to PMA that was prevented by Ro318220 (Fig. 6, *B* and *C*). A 30-min treatment with 1 nM PMA significantly increased H_2O_2 generation from Duox2/DuoxA2 co-transfected cells (data not shown). No increase of Duox1 phosphorylation could be observed after PMA treatment, and the inhibitor Ro318220 did not inhibit PMA-stimulated Duox1 activity (data not shown). These results suggest that physiologically PKC-α or -β1 isoforms participate in the phosphorylation and activation of Duox2 and not Duox1.

Regulation of H_2O_2 Generation in Human Thyroid Primary Cultures—In the functional assay, we found that Duox1 and Duox2 activities are both calcium-dependent but differentially regulated by PKA and PKC. To determine the physiological relevance of these results, we analyzed the modulation of H_2O_2 production in human thyrocytes under similar stimulation conditions. H_2O_2 measurements from primary cultures showed that basal H_2O_2 accumulation (0.31 ng of H_2O_2/μg of protein) was increased by ionomycin (4.08 ng of H_2O_2/μg of protein) and not by Fsk alone (Fig. 7*A*). Combining Fsk and ionomycin treatments significantly increased the H_2O_2 production to 7.16 ng of H_2O_2/μg of protein (Iono *versus* Iono+Fsk, $p < 0.001$), demonstrating a permissive effect of calcium rather an additive effect observed in the heterologous system (Fig. 2*E*). Ionomycin also increased the H_2O_2 amount in response to PMA to a similar extent (Iono *versus* Iono+PMA, $p < 0.001$). The 190-kDa mature form of Duox proteins was phosphorylated in basal condition and showed increased phosphorylation level after stimulation with Fsk or PMA as estimated by ^{32}P incorporation (Fig. 7*B*). This Duox phosphorylation was reproduced by 1 or 10 milliunits/ml of the thyrotropin hormone (TSH), concentrations described to stimulate either the adenylate cyclase-cAMP pathway or the phospholipase C-diacylglycerol-calcium cascade, respectively (27).

DISCUSSION

The biochemical function of hydrogen peroxide in thyroid hormone synthesis has been known for decades (18). A flavoprotein complex was predicted to produce directly H_2O_2 outside the cell with an activity mediated by NADPH and stimulated by calcium (10, 35, 39, 40). In 2000, the cloning of two cDNAs encoding novel calcium-dependent NADPH oxidases, Duox1 and Duox2, revealed the molecular nature of the presumed thyroid H_2O_2-generating system (1, 2, 11). However, functional studies on dual oxidases have been conducted only recently thanks to the discovery of their maturation factors, DuoxA1 and DuoxA2, allowing correct processing of Duox1–2 isoenzymes in heterologous systems (12, 13). In this work, we improved a DuoxA-based functional assay to compare the specific activities of Duox1 and Duox2, and we uncovered mechanisms of activation that discriminate between the two oxidase activities.

Each Duox protein possesses two canonical EF-hand motifs that are involved in the main regulation step exerted by calcium (2, 13, 34, 41). Co-expression of Duox/DuoxA proteins in Cos-7 cells reconstitutes an H_2O_2 generator with an activity acutely stimulated by an elevation of the intracellular calcium concentration. We have demonstrated that intact EF-hand sequences are required to maintain functional Duox proteins. Moreover,
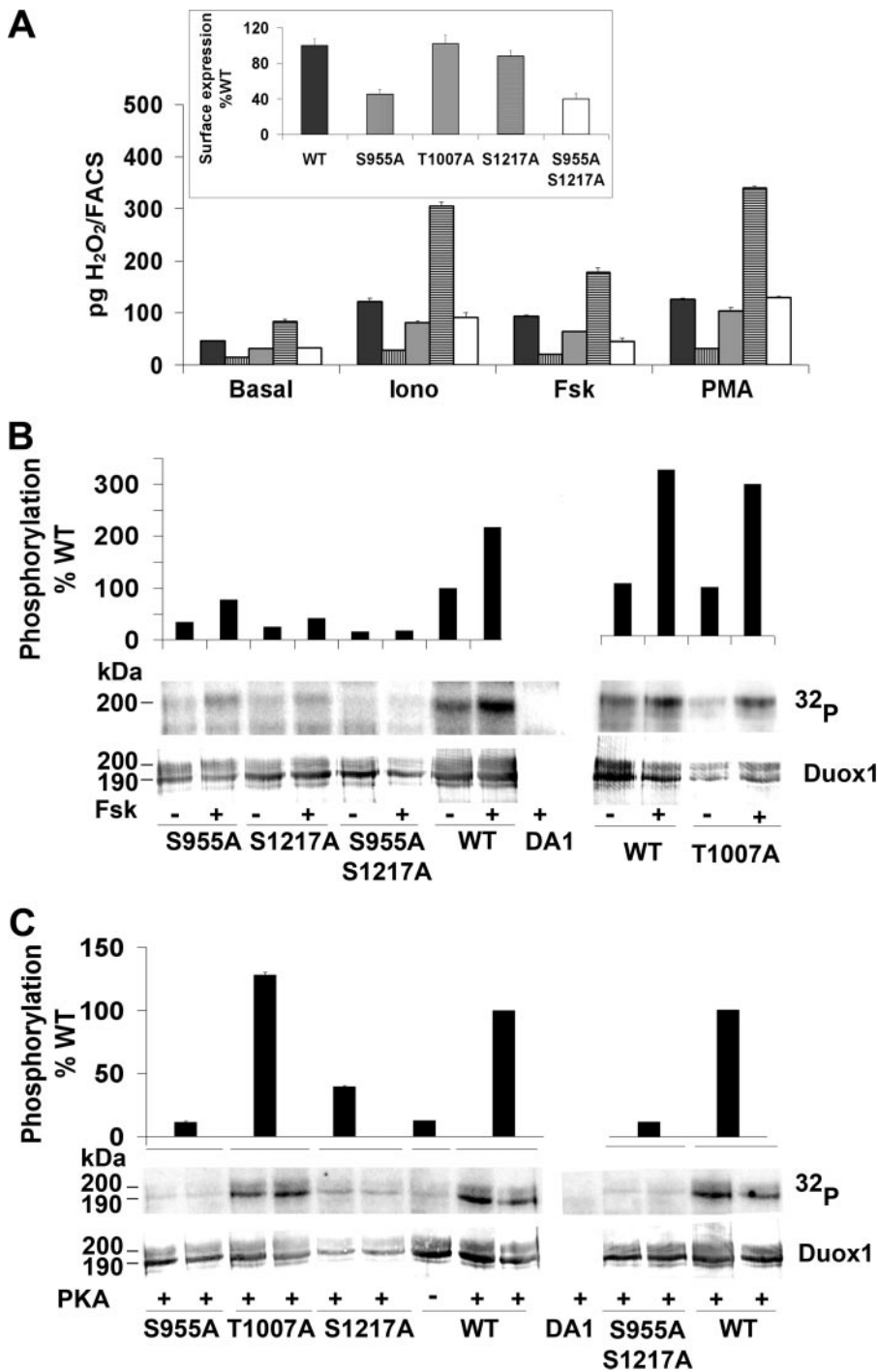
A

B

C

FIGURE 5. **Identification of PKA-mediated phosphorylation sites in Duox1.** *A*, Duox1 activity. Cos-7 cells expressing DuoxA1 in combination with WT (*black bars*), S955A (*vertically hatched bars*), T1007A (*gray bars*), S1217A (*horizontally hatched bars*), or S955A/S1217A (*open bars*) Rho-HA-Duox1 were stimulated for 2.5 h with 1 μM ionomycin (*Iono*), 1 μM Fsk, or 5 μM PMA and H$_2$O$_2$ accumulation normalized to Duox membrane expression. The *inset* shows the cell surface expression for each constructs relative to WT Duox1. The graph corresponds to one representative experiment from four independent experiments (means $\pm$ S.D., $n = 2$). *B*, Duox1 phosphorylation. Cells expressing DuoxA1 with WT or mutant Rho-HA-Duox1 were ^{32}P-labeled and treated for 30 min with either 1 μM Fsk (+) or solvent (−). In the *top panel*, relative densitometry of phosphorylated Duox1 corrected to the total Duox1 immunoprecipitated (non stimulated WT Duox1 considered as 100%). *C*, *in vitro* phosphorylation of Duox1 by PKA. Each construct was tested in duplicate. The relative Duox1 phosphorylation corrected to the total amount of Duox1 is showed on the *top* of the figure.

centrations. This effect might be explained by the differences in the amino acid sequence of the Duox1 second EF-hand motif.

Recent reports have shown that, in addition to calcium, the Nox5 enzymatic activity is also regulated through PKC-mediated phosphorylations on serine and threonine residues enhancing its sensitivity to calcium (42). Using radioactive phosphorus incorporation and anti-phospho-PKA substrate antibody, we demonstrated that Duox1 is also a phosphoprotein. The enzyme is constitutively phosphorylated, and activation of the PKA pathway increases its phosphorylation state as well as its activity. Immature Duox1–2 proteins generate essentially superoxide inside the cell and become H$_2$O$_2$ generators only at the cell surface (41). In transfected cells, *in vivo* ^{32}P incorporation shows that mainly the mature form of Duox1 is phosphorylated in basal and stimulated conditions, even if the immature form of Duox1 is more abundant (Fig. 5*B*). These data suggest that, in intact cells, Duox isoenzymes might undergo conformational changes during their processing from the endoplasmic reticulum to the plasma membrane modifying the accessibility of key residues to the kinase. In *in vitro* PKA phosphorylation experiments, these amino acids could be artificially demasked by detergents showing elevated phosphorylation intensity for the immature form of Duox1 (Fig. 5*C*).

Mass spectrometry analyses revealed Duox1 phosphopeptides containing the residues Ser[955] and Ser[1217] in co-transfected Cos-7 cells in response to Fsk. Systematic mutations of potential PKA-mediated phosphorylation sites have identified Ser[955] and Ser[1217] as major residues responsible for the basal phosphorylation state of Duox1. These two serines are conserved among human, dog, pig, mouse, and rat species. However, rendering these amino acids non-phosphorylatable reveals distinct effects on Duox1 specific activity. The S1217A variant presents higher constitutive activity than the WT enzyme and still responds to cAMP cascade
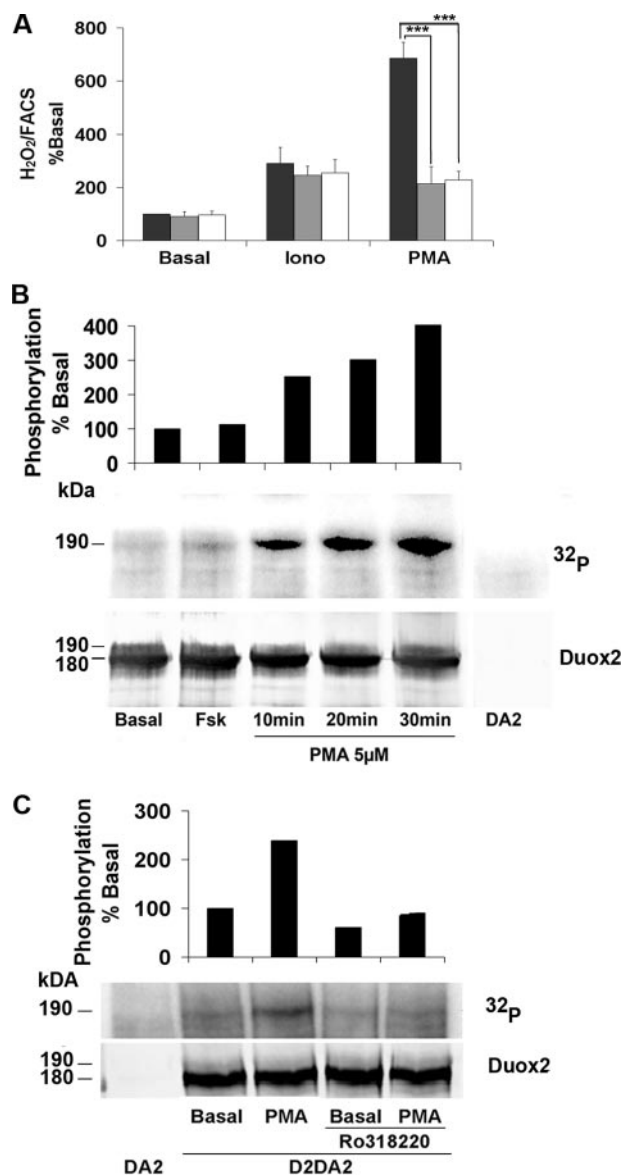
whereas the two dual oxidases exhibit similar activity at low ionomycin concentration (1 μM), Duox1 seems to be more efficient than Duox2 in cells treated with higher ionomycin con-

FIGURE 6. **PMA stimulates the activity and phosphorylation of Duox2.** *A*, cells co-transfected with HA-Duox2/DuoxA2 were preincubated 30 min in Krebs-Ringer-Hepes medium containing vehicle (*black bars*) or PKC inhibitors: 1 μM Ro318220 (*gray bars*) or 1 μM Gö6976 (*open bars*) before 2.5 h of stimulation with 1 μM ionomycin (*Iono*) or 1 nM PMA. H_2O_2 accumulation was normalized to Duox2 expression at the plasma membrane. The level of H_2O_2 is represented as a percentage of the value obtained in basal condition without PKC inhibitor (means ± S.D., *n* = 6). Statistically significant inhibition is indicated. ***, *p* < 0.001. *B*, phosphorylation by ^{32}P incorporation measured after 10, 20, or 30 min of treatment with 5 μM PMA. On the *top* of the Western blot, the relative amount of phosphorylated Duox2 corrected to total Duox2 protein (basal phosphorylation was considered as 100%). *C*, inhibition of PMA-mediated Duox2 phosphorylation by Ro318220. The cells were preincubated or not with 1 μM Ro318220 before stimulated with 100 nM PMA. Total Duox2 proteins were detected with anti-Duox antibody, and the relative Duox2 phosphorylation corrected to total Duox2 protein is represented at the *top* of the figure (basal phosphorylation without PKC inhibitor was considered as 100%).

FIGURE 7. **H_2O_2 measurement and Duox phosphorylation in human thyrocytes.** *A*, cells were incubated 90 min at 37 °C with 1 μM ionomycin (*Iono*), 10 μM Fsk, or 5 μM PMA. The peroxide production was normalized to the total amount of proteins. The graphs show means ± S.D. of three independent experiments performed in duplicate (***, *p* < 0.001). *B*, Duox1–2 phosphorylation after stimulation by TSH, Fsk, and PMA. Thyrocytes were stimulated 30 min with 1 milliunits/ml TSH or 10 μM Fsk or 5 min with 10 milliunits/ml TSH or 5 μM PMA. Quantification of Duox phosphorylation corrected to total immunoprecipitated protein represented at the *top*. Basal condition performed in duplicate.

hyperactivity of the mutant S1217A was more surprising and suggests an inhibitory effect on the overall Duox1 activity driven by its phosphorylation state. Our hypothesis is that in resting cells, constitutive phosphorylation on Ser[1217] restrains the enzyme to limit peroxide generation, whereas PKA-mediated phosphorylation on Ser[955] stimulates Duox1-dependent H_2O_2 generation. Absence of phosphorylation on this residue in the S955A variant would decrease its sensitivity to calcium, explaining its lower basal activity. Combination of S955A and S1217A leads to a Duox1 phospho-null mutant with WT-like constitutive activity but without response to PKA stimulation. However, we cannot exclude the possibility that these mutations could also be associated with conformational changes, inactivating the enzyme as suggested by low cell surface expression of the S955A and S955A/S1217A proteins.

Duox2/DuoxA2 co-transfected cells treated with nanomolar concentrations of PMA show increased H_2O_2 generation associated with PMA-mediated Duox2 phosphorylations. Duox2 enzyme is 1,000 times more sensitive to PMA than Duox1, suggesting that in physiological conditions, the resting levels of diacylglycerol combined with basal calcium concentration would be sufficient to stimulate Duox2 but not Duox1. Therefore, Duox2 would be the predominant enzyme in the thyroid conferring constitutive activity to the system. A survey of the Duox2 primary sequence reveals 11 (S/T)X(R/K) motifs as potential target sites for PKC. Among them, six are not conserved in Duox1 and constitute good candidates for PKC-mediated phosphorylations. Their implication on Duox2 activity will be investigated.

The crucial role of Duox2 in the thyroid hormone biosynthesis has been demonstrated in permanent congenital hypothyroidism caused by bi-allelic *DUOX2* gene mutations (20–25). Mono-allelic inactivation of *DUOX2* gene has also been linked

activation, whereas the S955A substitution decreases basal and Fsk-stimulated Duox1 activity. These results demonstrate that serine 955 is the crucial residue positively regulating Duox1 activity through PKA-mediated phosphorylation. It could increase the sensitivity of Duox1 to lower level of intracellular calcium as has been demonstrated for Nox5 enzyme (42). The
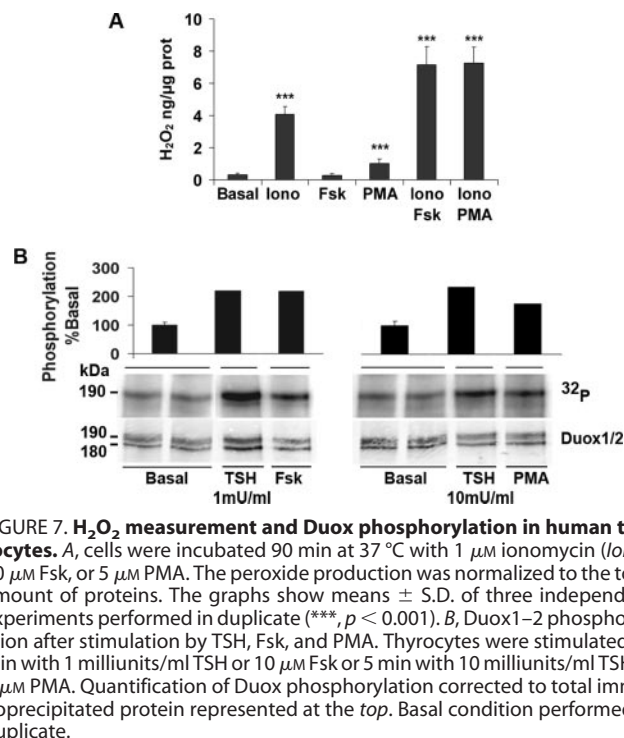
to milder and transient cases of neonatal hypothyroidism (43). Recently, *DUOXA2* bi-allelic mutations in a patient suffering from permanent dyshormonogenesis have been described, reinforcing the role of Duox2/DuoxA2 in thyroid metabolism (44). However, the role of existing Duox1/DuoxA1 beside Duox2 proteins in the same tissue remains obscure. Complete inactivation of *DUOX2* generally leads to partial iodide organification defect meaning that Duox1/DuoxA1 could compensate the impairment of Duox2 (13, 21, 22, 24, 25). Recently, we have demonstrated that Duox1 is the main source of hydrogen peroxide in the rat thyroid cell line: PCCl3 (45). Our experiments in human thyroid cells showing that elevation of intracellular cAMP concentration activates hydrogen peroxide production reinforce the concept of a thyroid function for Duox1. However, this effect is observed only in combination with ionomycin treatment. During the completion of this manuscript, Pacquelet *et al.* (46) have demonstrated an inhibitory effect on Duox activity by the Nox1 co-activator, NOXA1, which is relieved by calcium binding on Duox. They showed that cell lines devoid of NOXA1 protein exhibit high basal activity of Duox compared with the airway cells. The absence of Noxa1 in Cos-7 cells could explain why Fsk and PMA are able to stimulate Duox activity independently of ionomycin treatment. The NOXA1 transcript has been detected in thyrocytes (47), where it might also act as a down-regulator of the thyroid H_2O_2-generating system.

In humans, thyroid metabolism is under the control of the thyrotropin hormone (TSH) through its G protein-coupled receptor linked to adenylate cyclase-cAMP and phospholipase C-diacylglycerol-calcium cascades (26, 27, 48–50). Because Duox2 transcript is 2 to 5 times more abundant than Duox1 (51), we propose the following model in which the Duox2 system would ensure the constitutive tonic generation of H_2O_2 to make use of any available iodide. When thyroid hormone levels in the blood decrease, TSH concentration augments and triggers the release of both G_s and G_q proteins followed by intracellular increase of cAMP, diacylglycerol, and Ca^{2+} concentrations. The latter constitute the primary activator of the dual oxidase function, which is sustained by additional phosphorylations mediated by PKA for Duox1 and PKC for Duox2. Duox1 would represent the emergency program revealed in the case of hypothyroidism with partial iodide organification defect linked to inactive mutated Duox2. Nevertheless, Duox1 cannot fully take over the impairment of Duox2, probably because of too low protein expression.

In conclusion, we have used molecular approaches to characterize the mechanisms regulating the function of Duox1 and Duox2 proteins. We have demonstrated that the activity of the two dual oxidases is controlled via two different phosphorylation pathways, and we provide the first experimental argument in favor of a thyroid function for the Duox1 enzyme.

REFERENCES

1. Dupuy, C., Ohayon, R., Valent, A., Noel-Hudson, M. S., Deme, D., and Virion, A. (1999) *J. Biol. Chem.* **274,** 37265–37269
2. De Deken, X., Wang, D., Many, M. C., Costagliola, S., Libert, F., Vassart, G., Dumont, J. E., and Miot, F. (2000) *J. Biol. Chem.* **275,** 23227–23233
3. Lambeth, J. D. (2004) *Nat. Rev. Immunol.* **4,** 181–189
4. Babior, B. M. (1999) *Blood* **93,** 1464–1476
5. Banfi, B., Clark, R. A., Steger, K., and Krause, K. H. (2003) *J. Biol. Chem.* **278,** 3510–3513
6. Takeya, R., Ueno, N., Kami, K., Taura, M., Kohjima, M., Izaki, T., Nunoi, H., and Sumimoto, H. (2003) *J. Biol. Chem.* **278,** 25234–25246
7. Sumimoto, H., Miyano, K., and Takeya, R. (2005) *Biochem. Biophys. Res. Commun.* **338,** 677–686
8. Cheng, G., Ritsick, D., and Lambeth, J. D. (2004) *J. Biol. Chem.* **279,** 34250–34255
9. Banfi, B., Malgrange, B., Knisz, J., Steger, K., Dubois-Dauphin, M., and Krause, K. H. (2004) *J. Biol. Chem.* **279,** 46065–46072
10. Dupuy, C., Kaniewski, J., Deme, D., Pommier, J., and Virion, A. (1989) *Eur. J. Biochem.* **185,** 597–603
11. De Deken, X., Wang, D., Dumont, J. E., and Miot, F. (2002) *Exp. Cell Res.* **273,** 187–196
12. Grasberger, H., and Refetoff, S. (2006) *J. Biol. Chem.* **281,** 18269–18272
13. Grasberger, H., De Deken, X., Miot, F., Pohlenz, J., and Refetoff, S. (2007) *Mol. Endocrinol.* **21,** 1408–1421
14. Geiszt, M., Witta, J., Baffi, J., Lekstrom, K., and Leto, T. L. (2003) *FASEB J.* **17,** 1502–1504
15. El Hassani, R. A., Benfares, N., Caillou, B., Talbot, M., Sabourin, J. C., Belotte, V., Morand, S., Gnidehou, S., Agnandji, D., Ohayon, R., Kaniewski, J., Noel-Hudson, M. S., Bidart, J. M., Schlumberger, M., Virion, A., and Dupuy, C. (2005) *Am. J. Physiol.* **288,** G933–G942
16. Ha, E. M., Oh, C. T., Bae, Y. S., and Lee, W. J. (2005) *Science* **310,** 847–850
17. Dumont, J. E. (1971) *Vitam. Horm.* **29,** 287–412
18. Nunez, J., and Pommier, J. (1982) *Vitam. Horm.* **39,** 175–229
19. Corvilain, B., Van Sande, J., Laurent, E., and Dumont, J. E. (1991) *Endocrinology* **128,** 779–785
20. Moreno, J. C., Bikker, H., Kempers, M. J., van Trotsenburg, A. S., Baas, F., de Vijlder, J. J., Vulsma, T., and Ris-Stalpers, C. (2002) *N. Engl. J. Med.* **347,** 95–102
21. Vigone, M. C., Fugazzola, L., Zamproni, I., Passoni, A., Di Candia, S., Chiumello, G., Persani, L., and Weber, G. (2005) *Hum. Mutat.* **26,** 395
22. Varela, V., Rivolta, C. M., Esperante, S. A., Gruneiro-Papendieck, L., Chiesa, A., and Targovnik, H. M. (2006) *Clin. Chem.* **52,** 182–191
23. Pfarr, N., Korsch, E., Kaspers, S., Herbst, A., Stach, A., Zimmer, C., and Pohlenz, J. (2006) *Clin. Endocrinol.* **65,** 810–815
24. Ohye, H., Fukata, S., Hishinuma, A., Kudo, T., Nishihara, E., Ito, M., Kubota, S., Amino, N., Ieiri, T., Kuma, K., and Miyauchi, A. (2008) *Thyroid* **18,** 561–566
25. Maruo, Y., Takahashi, H., Soeda, I., Nishikura, N., Matsui, K., Ota, Y., Mimura, Y., Mori, A., Sato, H., and Takeuchi, Y. (2008) *J. Clin. Endocrinol. Metab.* **93,** 4261–4267
26. Raspe, E., Laurent, E., Andry, G., and Dumont, J. E. (1991) *Mol. Cell. Endocrinol.* **81,** 175–183
27. Corvilain, B., Laurent, E., Lecomte, M., Vansande, J., and Dumont, J. E. (1994) *J. Clin. Endocrinol. Metab.* **79,** 152–159
28. Vlaeminck-Guillem, V., Ho, S. C., Rodien, P., Vassart, G., and Costagliola, S. (2002) *Mol. Endocrinol.* **16,** 736–746
29. Roger, P. P., Hotimsky, A., Moreau, C., and Dumont, J. E. (1982) *Mol. Cell. Endocrinol.* **26,** 165–176
30. Roger, P., Taton, M., van Sande, J., and Dumont, J. E. (1988) *J. Clin. Endocrinol. Metab.* **66,** 1158–1165
31. Benard, B., and Brault, J. (1971) *Union Med. Can.* **100,** 701–705
32. Minamide, L. S., and Bamburg, J. R. (1990) *Anal. Biochem.* **190,** 66–70
33. Shevchenko, A., Tomas, H., Havlis, J., Olsen, J. V., and Mann, M. (2006) *Nat. Protoc.* **1,** 2856–2860
34. Luxen, S., Belinsky, S. A., and Knaus, U. G. (2008) *Cancer Res.* **68,** 1037–1045
35. Dupuy, C., Deme, D., Kaniewski, J., Pommier, J., and Virion, A. (1988)

FEBS Lett. **233,** 74–78

36. Banfi, B., Tirone, F., Durussel, I., Knisz, J., Moskwa, P., Molnar, G. Z., Krause, K. H., and Cox, J. A. (2004) *J. Biol. Chem.* **279,** 18583–18591

37. Uhler, M. D., and McKnight, G. S. (1987) *J. Biol. Chem.* **262,** 15202–15207

38. Buchler, W., Meinecke, M., Chakraborty, T., Jahnsen, T., Walter, U., and Lohmann, S. M. (1990) *Eur. J. Biochem.* **188,** 253–259

39. Dupuy, C., Virion, A., Hammou, N. A., Kaniewski, J., Deme, D., and Pommier, J. (1986) *Biochem. Biophys. Res. Commun.* **141,** 839–846

40. Dupuy, C., Virion, A., Ohayon, R., Kaniewski, J., Deme, D., and Pommier, J. (1991) *J. Biol. Chem.* **266,** 3739–3743

41. Ameziane-El-Hassani, R., Morand, S., Boucher, J. L., Frapart, Y. M., Apostolou, D., Agnandji, D., Gnidehou, S., Ohayon, R., Noel-Hudson, M. S., Francon, J., Lalaoui, K., Virion, A., and Dupuy, C. (2005) *J. Biol. Chem.* **280,** 30046–30054

42. Jagnandan, D., Church, J. E., Banfi, B., Stuehr, D. J., Marrero, M. B., and Fulton, D. J. (2007) *J. Biol. Chem.* **282,** 6494–6507

43. Moreno, J. C., and Visser, T. J. (2007) *Endocr. Dev.* **10,** 99–117

44. Zamproni, I., Grasberger, H., Cortinovis, F., Vigone, M. C., Chiumello, G., Mora, S., Onigata, K., Fugazzola, L., Refetoff, S., Persani, L., and Weber, G. (2008) *J. Clin. Endocrinol. Metab.* **93,** 605–610

45. Rigutto, S., Hoste, C., Dumont, J. E., Corvilain, B., Miot, F., and De Deken, X. (2007) *Exp. Cell Res.* **313,** 3892–3901

46. Pacquelet, S., Lehmann, M., Luxen, S., Regazzoni, K., Frausto, M., Noack, D., and Knaus, U. G. (2008) *J. Biol. Chem.* **283,** 24649–24658

47. Geiszt, M., Lekstrom, K., Witta, J., and Leto, T. L. (2003) *J. Biol. Chem.* **278,** 20006–20012

48. Allgeier, A., Offermanns, S., van Sande, J., Spicher, K., Schultz, G., and Dumont, J. E. (1994) *J. Biol. Chem.* **269,** 13733–13735

49. D'Arcangelo, D., Silletta, M. G., Di Francesco, A. L., Bonfitto, N., Di Cerbo, A., Falasca, M., and Corda, D. (1995) *J. Clin. Endocrinol. Metab.* **80,** 1136–1143

50. Vassart, G., Desarnaud, F., Duprez, L., Eggerickx, D., Labbe, O., Libert, F., Mollereau, C., Parma, J., Paschke, R., Tonacchera, M., Vanderhaeghen, P., van Sande, J., Dumont, J. E., and Parmentier, M. (1995) *Ann. N. Y. Acad. Sci.* **766,** 23–30

51. Pachucki, J., Wang, D., Christophe, D., and Miot, F. (2004) *Mol. Cell. Endocrinol.* **214,** 53–62